Dioxygen Reduction by *bo*-Type Quinol Oxidase from *Escherichia coli* Studied by Submillisecond-Resolved Freeze−Quench EPR Spectroscopy†

Koji Matsuura,‡ Shiro Yoshioka,‡,§ Satoshi Takahashi,*,‡,|| Koichiro Ishimori,‡ Tatsushi Mogi,⊥,#,○ Hiroshi Hori,△ and Isao Morishima*,‡

Department of Molecular Engineering, Graduate School of Engineering, Kyoto University, Nishikyo, Kyoto 615-8510, Japan, Department of Biological Sciences, Graduate School of Science, University of Tokyo, Bunkyo, Tokyo 113-0033, Japan, ATP System Project, Exploratory Research for Advanced Technology, Japan Science and Technology Corporation, Midori, Yokohama 226-0026, Japan, Chemical Resources Laboratory, Tokyo Institute of Technology, Midori, Yokohama 226-8503, Japan, and Graduate School of Engineering Science, Osaka University, Toyonaka 560-8531, Japan

Received August 28, 2003; Revised Manuscript Received December 8, 2003

ABSTRACT: The mechanism of the dioxygen (O_2) reduction conducted by cytochrome *bo*-type quinol oxidase was investigated using submillisecond-resolved freeze−quench EPR spectroscopy. The fully reduced form of the wild-type enzyme (WT) with the bound ubiquinone-8 at the high-affinity quinone-binding site was mixed with an O_2-saturated solution, and the subsequent reaction was quenched at different time intervals from 0.2 to 50 ms. The EPR signals derived from the binuclear center and heme *b* were weak in the time domain from 0.2 to 0.5 ms. The signals derived from the ferric heme *b* and hydroxide-bound ferric heme *o* increased simultaneously after 1 ms, indicating that the oxidation of heme *b* is coupled to the formation of hydroxy heme *o*. In contrast, the enzyme without the bound ubiquinone-8 (ΔUbiA) showed the faster oxidation of heme *b* and the slower formation of hydroxy heme *o* than WT. It is interpreted that the F_I intermediate possessing ferryl−oxo heme *o*, cupric Cu_B, and ferric heme *b* is converted to the F_{II} intermediate within 0.2 ms by an electron transfer from the bound ubiquinonol-8 to ferric heme *b*. The conversion of the F_{II} intermediate to the hydroxy intermediate occurred after 1 ms and was accompanied by the one-electron transfer from heme *b* to the binuclear center. Finally, it is suggested that the hydroxy intermediate possesses no bridging ligand between heme *o* and Cu_B and is the final intermediate in the turnover cycle of cytochrome *bo* under steady-state conditions.

Cytochrome *bo*-type ubiquinol oxidase from *Escherichia coli* is a member of the heme−copper terminal oxidase superfamily and catalyzes the reduction of dioxygen to water with ubiquinol-8 (Q_8H_2)[1] in the cytoplasmic membrane (*1*−*3*). The enzyme utilizes the energy released during the dioxygen (O_2) reduction to pump protons across the membrane and establishes a protonmotive force to provide the driving force for the ATP synthesis and other cellular processes. The mechanism on the coupling of the oxygen activation and electron transfer with proton pumping has been extensively investigated.

Subunit I of cytochrome *bo* contains three redox-active metal centers, heme *b*, heme *o*, and Cu_B, whose coordinating ligands were determined by site-directed mutagenesis studies (*3*, *4*) and were confirmed by X-ray crystallographic studies (*5*). Heme *b* is biscoordinated by His106 and His421, and heme *o* is singly coordinated by His419. Cu_B is ligated by three histidines, His284, His333, and His334. Cu_B and heme *o* form the binuclear metal center, where O_2 is reduced to water. As shown for cytochrome *c* oxidase (*6*−*8*), another well-characterized member of the terminal oxidases (*9*, *10*), Nϵ2 of the imidazole ring at His284 is assumed to be covalently linked to Cϵ2 of the phenol ring at Tyr288 (*11*). A bound ubiquinone-8 (Q_8) at the high-affinity quinone-binding site located in the vicinity of heme *b* serves as the fourth redox center and mediates electron transfers from Q_8H_2 to heme *b* (*5*, *12*−*14*).

The accepted mechanism of the O_2 reduction reaction conducted by cytochrome *bo* can be summarized as follows

† This work was supported by Grants-in-Aid from the Ministry of Education, Culture, Sports, Science, and Technology in Japan (12002008 to I.M., 13680741 to H.H., 14658217 to K.I., and 15657027 to K.I., H.H., and S.T.) and from Exploratory Research for Advanced Technology, Japan Science and Technology Corp. (T.M.).

* To whom correspondence should be addressed. S.T.: tel, +81-6-6879-8615; fax, +81-6-6879-8616; e-mail, st@protein.osaka-u.ac.jp. I.M.: tel, +81-75-383-2535; fax, +81-75-383-2541; e-mail, morisima@mds.moleng.kyoto-u.ac.jp.

‡ Kyoto University.

§ Present address: Center for Integrative Bioscience, Okazaki National Research Institutes, Myodaiji, Okazaki, Aichi 444-8585, Japan.

|| Present address: Institute for Protein Research, Osaka University, Suita 565-0871, Japan.

⊥ University of Tokyo.

Japan Science and Technology Corp.

○ Tokyo Institute of Technology.

△ Osaka University.

[1] Abbreviations: EPR, electron paramagnetic resonance spectroscopy; Q_8, ubiquinone-8; Q_8H_2, a reduced form of ubiquinone-8; WT, cytochrome *bo* with the bound ubiquinone-8 at the high-affinity quinone-binding site; ΔUbiA, cytochrome *bo* without the bound ubiquinone-8; O_2, dioxygen; H_2O_2, hydrogen peroxide.

10.1021/bi0355490 CCC: $27.50
Published on Web 02/03/2004

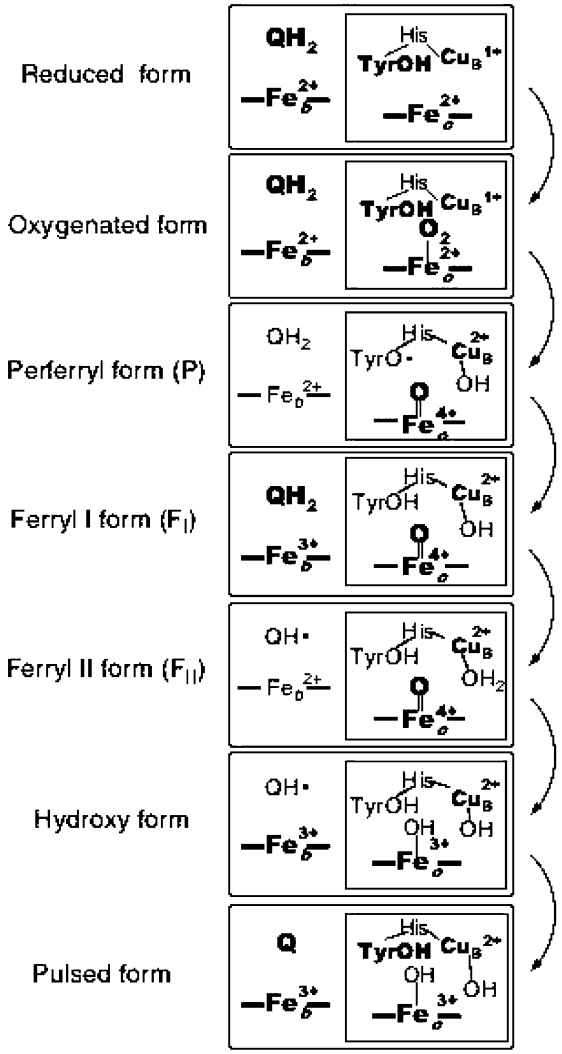

FIGURE 1: Catalytic mechanism for the O_2 reduction reaction conducted by the fully reduced cytochrome *bo*. The scheme describes the structures of the binuclear site (inner box) and the redox states of heme *b* and the bound ubiquinone-8 at the high-affinity quinone-binding site. The redox centers whose redox states are established are indicated in bold face type. The established ligands for heme *o* and Cu_B are also indicated in bold face type.

(Figure 1). Ferrous heme *o* in the fully reduced enzyme binds dioxygen and cleaves the O═O bond in the resultant oxy intermediate [Fe_o(II)−O_2] (*15*−*17*). The P intermediate is assumed to form next, which possesses ferryl−oxo heme *o* [Fe_o(IV)═O], cupric Cu_B, the cross-linked tyrosine radical, and ferrous heme *b* (*18*−*26*). The putative tyrosine radical is reduced by heme *b* in the F_I intermediate. The heme *b* site is reduced again by the bound Q_8H_2 to become the F_{II} intermediate and subsequently donates an electron to the binuclear center to make the hydroxy intermediate possessing hydroxide-bound ferric heme *o* [Fe_o(III)−OH] (*15*, *27*). Finally, the hydroxy intermediate is considered to decay to the pulsed form that shows a characteristic EPR signal at $g = 3.7$ due to the magnetic interaction between heme *o* and Cu_B (*28*). The mechanism is mainly based on the flow-flash optical absorption studies (*15*, *27*, *29*−*31*) and on the mechanism established for cytochrome *c* oxidase (*18*, *32*, *33*); however, the overlap of the absorption spectra for the two hemes precludes the detailed characterization of the reaction. In particular, the coordination structures of heme *o* and Cu_B and the redox states of the cross-linked tyrosine and Q_8 have not been directly observed in most of the intermediates.

To obtain information on the binuclear center in the P, F_I, and F_{II} intermediates of the O_2 reduction of cytochrome *bo*, the isoelectronic structures of the binuclear center for these intermediates have been prepared by reacting the pulsed enzyme with hydrogen peroxide (H_2O_2) (*21*, *34*−*37*). For example, a resonance Raman investigation demonstrated that both P and F intermediates prepared by the H_2O_2 reaction possess ferryl−oxo heme *o* and suggested the presence of the cross-linked tyrosine radical in the P intermediate (*21*). However, the reaction of the pulsed enzyme with H_2O_2 cannot provide information on the electron-transfer steps from the heme *b*/Q_8 system to the binuclear center. Furthermore, it was suggested that H_2O_2 produces nonphysiological radicals in the reactions of cytochrome *c* oxidase (*38*, *39*). It is desirable to investigate directly the short-lived intermediates generated in the O_2 reduction.

Electron paramagnetic resonance (EPR) spectroscopy is a powerful method that can characterize the valence and electronic states of the redox centers in cytochrome *bo* (*40*). The EPR signals for the low-spin heme *b* are distinct from those of the high-spin heme *o*. The signal for the cross-linked tyrosine radical was assigned on the basis of the D_4-Tyr-labeled cytochrome *c* oxidase (24) and on the model compound (*41*, *42*), although recent reports concluded that the tyrosine radical in the P intermediate prepared by the H_2O_2 reaction is EPR silent (*39*, *43*). The signal from Cu_B was also observed in the P_R intermediate (corresponding to F_I in Figure 1) of cytochrome *c* oxidase prepared by the triple-trapping method (*32*, *44*−*46*). However, it has been impossible to apply the EPR spectroscopy for the direct observation of the O_2 reduction reaction, since the conventional devices to freeze−trap reaction intermediates require a longer freezing time (5∼10 ms) compared to a single turnover (>500 s^{-1}) of cytochrome *bo* (*40*, *47*, *48*).

In this study, we used a novel freeze−quench device, which has the mixing-to-freezing time interval of 0.2 ms (*49*), and studied the trapped intermediates in the O_2 reduction reaction of cytochrome *bo* by EPR spectroscopy. We sought to observe the signals from the binuclear center in the reaction intermediates accessible by the new device. Furthermore, we compared the observed results for cytochrome *bo* with and without the bound ubiquinone to characterize the timing of the internal electron-transfer steps from the heme *b*/Q_8 system to the binuclear center.

MATERIALS AND METHODS

Purification of Cytochrome bo. The wild-type cytochrome *bo* with the bound Q_8 (WT) was isolated from GO103/pHN3795-1 as described previously (*50*). The bound Q_8-free enzyme (ΔUbiA) was purified from the ubiquinone biosynthesis mutant MU1227/pMFO4 (*12*). The HPLC analysis (*12*) indicated that the contents of protein-bound ubiquinone per enzyme (Q_8/*bo*) in WT and ΔUbiA are 1.0 and <0.01, respectively. The purified enzymes were dissolved in 100 mM Tris-HCl (pH 7.4) containing 0.1% sucrose monolaurate (SML; Mitsubishi-Kagaku Foods). All solutions used for the spectroscopic measurements had the same buffer and detergent composition.

Stopped-Flow Rapid Scanning Absorption Spectroscopy. Spectral changes in the reaction of the fully reduced enzyme with O_2 were measured using an OLIS rapid scan system (RSM-1000) equipped with a stopped-flow apparatus (UNISOKU). The mixing dead time of the apparatus was 3−5 ms. The sample solution containing 10 μM cytochrome *bo* was degassed and reduced with dithionite (~2.5 mM) in one of the stopped-flow reservoirs. The other reservoir was filled with the O_2-saturated buffer, which was mixed with the enzyme solution with a volume ratio of 1 to 1 at room temperature (~20 °C).

Rapid Freeze−Quench Device. The construction of the freeze−quench device was reported previously, which has the time interval of ~0.2 ms from mixing to freezing (*49*). In brief, two solutions continuously supplied from a syringe pump are mixed in the T-shaped microchannel and form a jet that flushes against rotary silver disks cooled at 77 K. Copper could not be used as the cooling disks due to contaminations of cupric copper signals (*49*). Special care was devoted to maintain the anaerobic condition of the device. The sample inlet was designed to attach a septum, through which the fully reduced enzyme can be transferred anaerobically. Before the introduction of the sample solution, the sample loop was washed twice with the degassed buffer and once with the buffer containing 5 mM dithionite, which was prepared anaerobically with the nitrogen-saturated buffer. The interval between the sample introduction and the freeze−quench procedure was kept within a few minutes.

The sample solution containing 500 μM cytochrome *bo* (250 μM for ΔUbiA) was degassed and reduced with dithionite (~2.5 mM). The fully reduced enzyme was introduced anaerobically into the sample loop and pushed toward the mixer by the buffer containing dithionite (~2.5 mM) introduced in one of the syringes. The other syringe was filled with the O_2-saturated buffer. The reduced enzyme and the O_2-saturated buffer were mixed with a volume ratio of 1 to 1 at room temperature (~20 °C), and freeze−quenched. The frozen powder in liquid nitrogen was manually collected and transferred to quartz EPR tubes or optical cells for spectroscopic measurements. To remove a small amount of frozen O_2, the EPR tubes were immersed in a liquid isopentane bath adjusted at ~120 K, evacuated, filled with nitrogen gas, and sealed (*49*).

Measurements of Absorption Spectra of Powdery Samples. Absorption spectra of the powdery frozen samples were recorded on a spectrophotometer (Lambda 19, Perkin-Elmer), which was modified to incorporate a cryostat (DN1704, Oxford) and frosted quartz windows (*49*). The intensity of the reference beam was reduced to compensate for the intensity decrease of the sample beam. The sample temperature (~120 K) was monitored by a thermocouple inserted directly in the cell. The slit width and the scan rate were 2 and 120 nm/min, respectively. Due to the difficulty to obtain accurate absorption spectra for the powdery samples, the intensity scales for the spectra presented in Figure 3C,D were arbitrary.

EPR Spectroscopy. EPR spectra were measured on a Varian E-12 spectrometer equipped with an Oxford ESR-900 liquid helium cryostat. The microwave frequency was X-band (9.22 GHz), and the measurements were carried out at 5, 15, and 35 K. The microwave power and modulation were 10 mW and 1 mT at 5 and 15 K and 0.2 mW and 0.2 mT at 35 K, respectively. To compare the signal intensities for the samples obtained at different freezing conditions, a set of intensity standards was obtained by freezing the resting sample at the respective conditions. By comparison of the intensities of ferric heme *b* in the kinetic spectra and in the reference spectra, the absolute spin contents for ferric heme *b* were estimated (closed circles in Figure 5). Since it is not possible to quantitate the total spin contents for hydroxy heme *o* due to spectral overlap, the changes in the relative spin contents of hydroxy heme *o* were estimated, setting the intensity for WT at 1 ms to 1 (open circles in Figure 5). The intensity data for WT were the average of two to four independent measurements (Figure 5A). The data for ΔUbiA were estimated from a single observation except for the datum at 0.4 ms that was observed twice (Figure 5B).

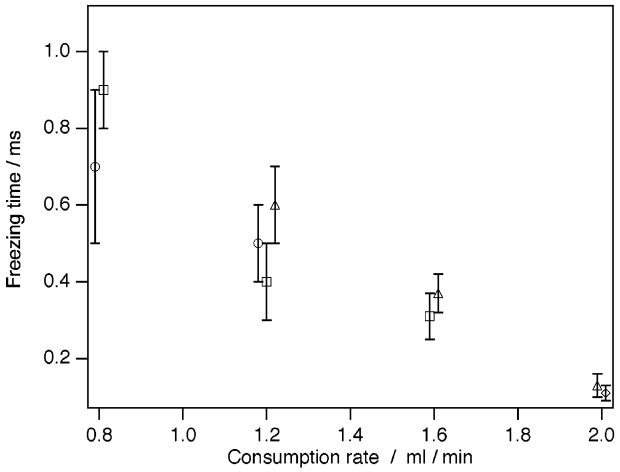

FIGURE 2: Estimated freezing times of the freeze−quench device operated at different sample consumption rates. The azide-binding reaction to 100 μM metmyoglobin at pH 7 was utilized as the reference reaction to estimate the freezing times that are the time intervals between the mixing and freezing. Circles, squares, triangles, and a diamond indicate the freezing times estimated with 100, 200, 400, and 800 mM sodium azide, respectively. The errors reflect the uncertainties in the estimated ratio of the azide-bound form (±5%). The *X*-axis indicates the sample consumption rate at the mixer. The distances between the mixer and the surfaces of the freezing blocks were fixed at 1 cm. The freezing times estimated using different azide concentrations are consistent.

RESULTS

Dead Times of the New Freeze−Quench Device. We previously reported the design and the performance of the new freeze−quench device with the mixing-to-freezing dead time of 0.2 ms (*49*). To establish the freezing conditions to trap the cytochrome *bo* reaction at different times, we systematically investigated the dead times of the device at different jet velocities and distances between the mixer and the cooling disks. We freeze−trapped the bimolecular binding reaction of sodium azide to metmyoglobin and observed the absorption spectra of the quenched samples. Upon the azide binding, the Soret peak of metmyoglobin changes from 408 to 420 nm, from which fractions of the azide-bound form were estimated (Figure 2). Using the bimolecular rate constant of the reaction at room temperature (7.0×10^3 s^{-1} M^{-1} at pH 7.0) (*51*) and the fractions, we estimated the quenching times at the different cooling conditions (Table 1). While the quenching times depend on

Table 1: Freezing Times (ms) of the Rapid Freeze−Quench Device Operated at Different Freezing Conditions Estimated Using Various Reference Reactions

	freezing conditions					
reference reactions	0.28 (5)[a]	0.56 (1)	0.8 (1)	1.2 (1)	1.6 (1)	2.0 (1)
metmyoglobin + NaN_3 (100 mM)	−[b]	−	0.7 ± 0.2[c]	0.5 ± 0.1	−	−
metmyoglobin + NaN_3 (200 mM)	−	−	0.9 ± 0.1	0.4 ± 0.1	0.31 ± 0.06	−
metmyoglobin + NaN_3 (400 mM)	−	−	−	0.6 ± 0.1	0.37 ± 0.05	0.13 ± 0.03
metmyoglobin + NaN_3 (800 mM)	−	−	−	−	−	0.11 ± 0.02
other reactions	50[d]	10[e]	−	−	−	0.2[f]
estimations	∼50	∼10	∼1.0	∼0.5	∼0.4	∼0.2

[a] The rates of sample consumption at the mixer (mL/min). The numbers in parentheses denote the distance from the mixer to the freezing blocks (in cm). [b] Not determined. [c] The estimated time intervals between mixing and freezing in milliseconds. The time intervals (t) were calculated using the formula $t = \ln[(1 - a)^{-1}]/(k[NaN_3])$ in which a, k, and $[NaN_3]$ represent the estimated ratio of the azide-bound form in the samples prepared by trapping the azide-binding reaction to metmyoglobin, the bimolecular rate constant between metmyoglobin and azide (7.0×10^3 s^{-1} M^{-1} at pH 7.0), and the concentration of azide (M) in the reference reactions, respectively. The errors reflect the uncertainties in the estimated ratio of the azide-bound form (±5%). [d] The estimated time interval from a reaction between metmyoglobin and 3.3 mM NaN_3. [e] The estiamted time interval from a reaction between metmyoglobin and 10 mM NaN_3. [f] The estimated time interval from a reaction between the deoxymyoglobin and 0.14 mM O_2 from ref *49*.

the reference reactions and should be considered as rough estimates (*49*), we confirmed that the freezing times from 0.2 to 50 ms can be systematically achieved using the device.

Dioxygen Reduction Reactions Monitored by Absorption Spectroscopy. To observe the O_2 reduction reaction by the fully reduced cytochrome *bo* in the millisecond time domain and to obtain the basis for understanding the data in the submillisecond time domain, we first utilized a stopped-flow rapid scanning method. The effect of the bound ubiquinone was investigated by comparing data obtained for the enzymes with (WT) and without the bound Q_8 (ΔUbiA). Time-resolved absorption spectra confirm that the oxidation of the reduced hemes *b* and *o* with the Soret peak at 427 nm was mostly completed in both WT and ΔUbiA within the dead time (3−5 ms) of our stopped-flow apparatus (Figure 3A,B). However, the increase of the broad Soret peak is slower and the peak maximum at 10 ms is red shifted in ΔUbiA, indicating the difference in the electronic structures of the hemes in WT and ΔUbiA at 10 ms.

To observe the spectral changes within the mixing dead time of the stopped-flow apparatus, we next trapped the reaction intermediates by the freeze−quench device and recorded the absorption spectra at the cryogenic temperature (∼120 K). Absorption spectra of WT and ΔUbiA frozen at 10 ms (Figure 3C,D) can be compared to the respective spectra of the stopped-flow experiments (Figure 3A,B). Considering the uncertainty in the freezing times and the spectral deformations caused by powdery samples, the spectra obtained at 10 ms by the two methods are consistent. Furthermore, the submillisecond data demonstrate the distinct difference in the kinetics of WT and ΔUbiA. The absence of the 427 nm peak in ΔUbiA at 0.5 and 1 ms reveals that the two hemes are mostly oxidized. In contrast, the 427 nm peak is still present in the spectra obtained at 0.5 and 1 ms for WT. These results are consistent with the previous flow−flash studies (*15*, *27*) and suggest that heme *b* rapidly donates an electron to the binuclear center and is rereduced by the bound Q_8H_2 in WT. In contrast, the oxidized heme *b* cannot be rereduced in ΔUbiA due to the absence of the bound Q_8H_2. Thus, we were successful in freeze−trapping the cytochrome *bo* reaction for the first time with the submillisecond time resolution.

Changes in Hemes b and o Monitored by Freeze−Quench EPR Spectroscopy. To monitor the coordination and valence states of the redox centers, the O_2 reduction by the fully reduced enzyme was studied by the freeze−quench EPR spectroscopy in the time region from 0.2 to 50 ms. If signals originated from ferric heme *o*, Cu_B^{2+}, and the tyrosine radical were to be observed, they are expected to appear at 5 K due to the broadening of these signals at the higher temperature. At 5 K, a signal at around $g = 6$, which is assigned to ferric heme *o* lacking the magnetic interactions with Cu_B, appears

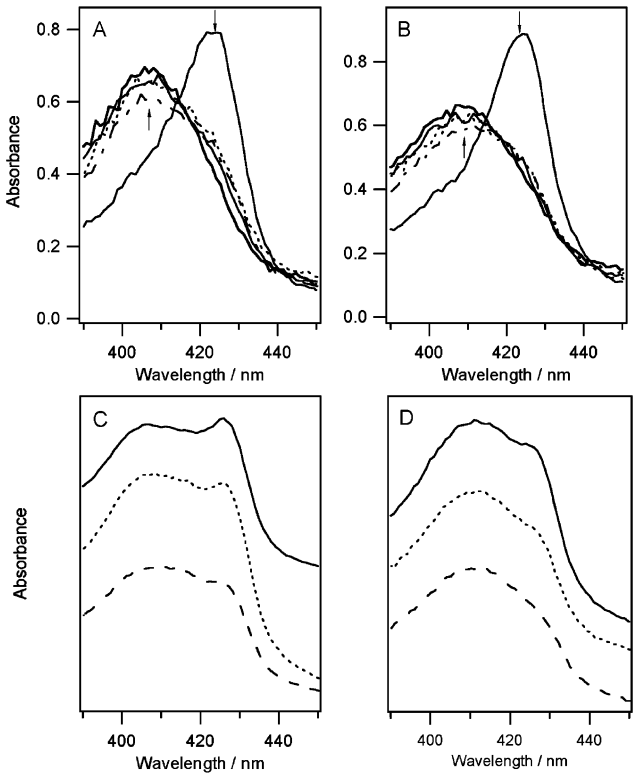

FIGURE 3: Kinetic absorption spectra for the reaction of cytochrome *bo* with O_2 obtained using the stopped-flow and freeze−quench methods. Panels A and B show the stopped-flow scans for the reactions of WT and ΔUbiA at 25 °C, respectively. Solid, dashed, dotted, solid, and bold solid curves are the spectra recorded at 0 (corresponding to the spectrum before mixing), 6, 8, 10, and 50 ms, respectively. Panels C and D show the kinetic absorption spectra for the freeze−quenched WT and ΔUbiA, respectively, observed at the cryogenic temperature. The estimated time intervals between mixing and freezing are 0.5 (solid curve), 1 (dotted curve), and 10 ms (dashed curve).

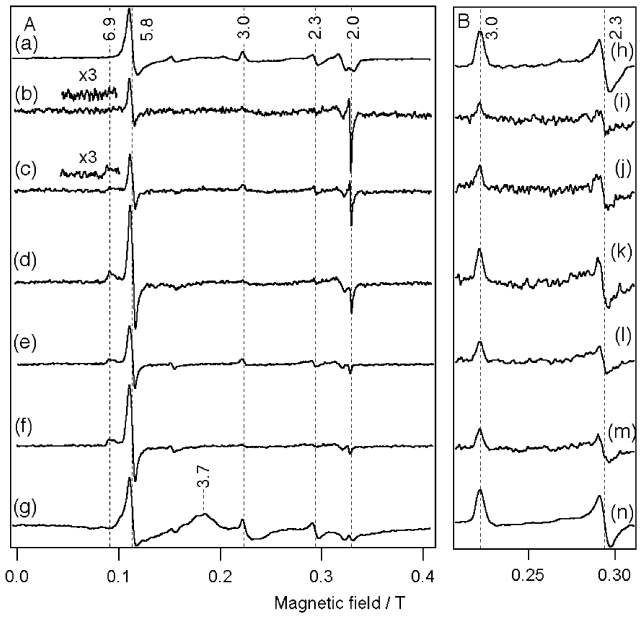

FIGURE 4: Time-resolved EPR spectra for the reaction of WT cytochrome *bo* with O_2. Panels A and B show the spectra recorded at 5 and 15 K, respectively. Traces a and h (resting form) and traces g and n (pulsed form) show the spectra for static samples. Traces b−f of panel A show the spectra recorded at 5 K for the samples quenched at 0.2, 0.4, 1, 10, and 50 ms after mixing the fully reduced WT with O_2, respectively. Traces i−m of panel B were recorded for the corresponding samples at 15 K. All spectra were obtained at 10 mW of microwave power with 1 mT of modulation. The intensities of the spectra were normalized on the basis of the reference spectra of the resting sample frozen at the respective conditions.

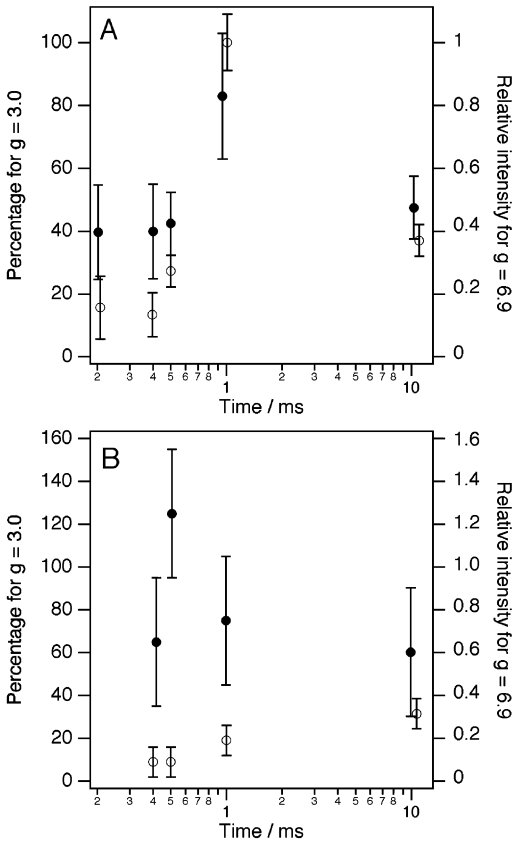

FIGURE 5: Time-dependent changes in the intensities of the EPR signals observed in the O_2 reduction of cytochrome *bo*. (A) Changes in the absolute contents of ferric heme *b* (closed circle, left scale) and the relative contents of hydroxy heme *o* (open circle, right scale) for WT. (B) Changes in the absolute contents of ferric heme *b* (closed circle, left scale) and the relative contents of hydroxy heme *o* (open circle, right scale) for ΔUbiA.

for all of the samples (*52*) (Figure 4A). Similarly, a signal at $g = 2.0$ corresponds to a trace amount of free radicals. Except for these signals and a weak signal from heme *b* at $g = 3.0$, no distinct signal was observed at 0.2 and 0.4 ms. A signal at $g = 6.9$, which is assignable to a ferric hydroxide-bound heme *o* (*53*), starts to appear at 0.4 ms. We could not observe any signals from the cross-linked tyrosine radical and Cu_B(II) even with the smaller modulation width (0.5 mT) and with the higher microwave power (∼50 mW) (data not shown). Thus, the only EPR signal from the binuclear center was the hydroxide-bound heme *o* that begins to appear at 0.4 ms. A rate constant for the increase can be roughly estimated as 500−700 s^{-1} from the intensity plot of the hydroxy heme *o* (Figure 5A).

In contrast to the signals from the binuclear center, the heme *b* signals are more sensitively observed at 15 K. The redox states of heme *b* can be monitored using the $g_z = 3.0$ and $g_y = 2.3$ signals at 15 K of the ferric low-spin heme *b* (Figure 4B). The time-dependent plot of the absolute contents of heme *b*, estimated on the basis of the reference spectra of the resting sample prepared in the respective freezing conditions, indicates that the contents were 25−55% at 0.2 ms but reached 60−100% at ∼1 ms (Figure 5A). This behavior is reminiscent of the intensity change observed for the hydroxy heme *o* ($g = 6.9$) at 5 K. It is apparent that the intensity increase for the two signals coincides in the time domain from 0.4 to 1 ms, indicating that the major changes in the valence states of hemes *b* and *o* occur in the same kinetic phase.

We next observed the EPR spectra of ΔUbiA at 0.4, 0.5, 1, and 10 ms to examine the effect of eliminating the bound Q_8H_2 on the electron-transfer steps from heme *b* to heme *o*. The signals observed in the time-resolved spectra were similar to those of the WT enzyme (Figure 6). The $g = 6.9$ signal of the hydroxy heme *o* appeared at 10 ms, but no signals from Cu_B and the cross-linked tyrosine were observed. A closer examination of the signal intensities, however, suggests the slower increase of the hydroxy heme *o* and the faster increase of the ferric heme *b* in ΔUbiA. The intensity plots for the two signals confirm the distinct difference between ΔUbiA and WT (Figure 5). Together with the optical absorption data showing the absence of the 427 nm peak in ΔUbiA (Figure 3), we conclude that ΔUbiA exhibits the faster and slower appearances of the ferric heme *b* and the hydroxy heme *o* signals, respectively, than those of WT.

Detection of the Ubisemiquinone Radical. To examine the contents of the ubisemiquinone radical, we recorded EPR spectra at 35 K. The ubisemiquinone radical is weak at the lower temperatures due to the facile power saturation. A radical signal at $g = 2$ in the WT spectrum showed a weak hyperfine splitting as reported previously in the redox potentiometric studies (*54*, *55*) and can be assigned to the ubisemiquinone radical. The signal did not change its intensity significantly at the freezing times from 0.2 to 50 ms (Figure 7). The spin content of the ubisemiquinone radical

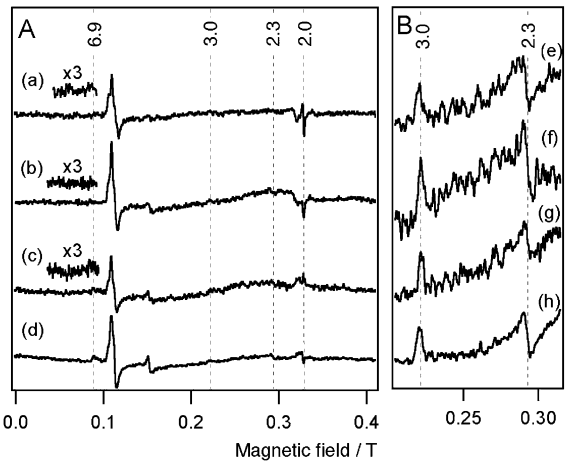

FIGURE 6: Time-resolved EPR spectra for the O_2 reduction reaction by ΔUbiA. Traces a−d in panel A were recorded at 5 K for the samples quenched at 0.4, 0.5, 1, and 10 ms after mixing the reduced ΔUbiA with O_2. Traces e−h of panel B were recorded for the corresponding samples at 15 K. All spectra were obtained at a microwave power of 10 mW with a modulation of 1 mT.

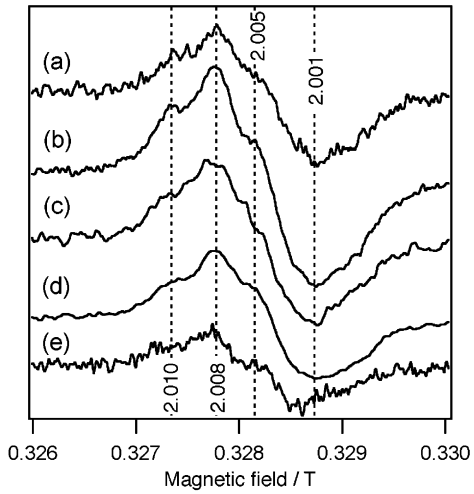

FIGURE 7: EPR spectra at 35 K for the O_2 reduction by WT and ΔUbiA. Traces a−d show the spectra for the samples quenched at 0.4, 0.5, 1, and 10 ms, respectively, after mixing the fully reduced WT with O_2. Trace e shows the spectrum for ΔUbiA quenched at 0.4 ms. All spectra were recorded at 0.2 mW of microwave power and 0.2 mT of modulation.

at 10 ms was estimated to be only ∼3% of that of ferric heme *b*. While a similar signal was observed for ΔUbiA with the reduced intensity (∼1/2.5 of WT), it should be derived from the enzyme moiety, since the bound ubiquinone is absent in ΔUbiA. Thus, the bound ubiquinone is mostly EPR silent in WT under our experimental conditions.

DISCUSSION

Dioxygen Reduction by Cytochrome bo with the Bound Q_8. Before interpreting the time-resolved data, we note that the F_I intermediate in Figure 1, possessing ferric heme *b*, ferryl−oxo heme *o*, and cupric Cu_B, corresponds to "P_R" in the reaction scheme of cytochrome *c* oxidase proposed by Morgan et al. (*32*). We, however, adopted "F_I" from the scheme proposed by Sucheta et al. (*33*). The P and F intermediates have been considered as two- and one-electron oxidized species from the ferric−cupric binuclear center, respectively (*56*, *57*). The binuclear center including the cross-linked tyrosine in both F_I and F_{II} is one electron oxidized than that of the pulsed form and is rather consistent with the convention of "F". Except for the difference in the nomenclature, the reaction scheme in Figure 1 is consistent with the model proposed by Morgan et al. (*32*) and with the model proposed for cytochrome *bo* (*15*).

We assign that the WT enzyme quenched at 0.2 and 0.4 ms is mostly in the F_{II} intermediate of Figure 1. It has been indicated that the initial several steps of the cytochrome *bo* reaction are complete within 0.2 ms. Flow−flash studies demonstrated the decay of the oxygenated intermediate within 100 μs (*15*, *29*, *30*, *50*). A time-resolved resonance Raman study identified the Fe(IV)═O stretching vibration at 780 cm^{-1} in the time domain from 20 to 40 μs (*17*), which was assigned as the F intermediate in the reaction of the pulsed enzyme with H_2O_2 (*21*). Furthermore, the ferric heme *b* in F_I was demonstrated to be rereduced by the bound Q_8H_2 to make F_{II} with a time constant of ∼0.6 ms (*15*, *27*). The current data indicate that a large fraction of heme *b* in the samples quenched at 0.2 and 0.4 ms is in the ferrous state and are consistent with the assignment to the F_{II} intermediate. To explain the small amount of the ubisemiquinone radical, we suggest that the putative ubisemiquinone radical in F_{II} is unstable and might be reduced by excess dithionite in the reaction mixture before the quenching procedure.

We next assign that the quenched sample after 1 ms is in the hydroxy intermediate. In the freeze−quenched EPR spectra after 0.4 ms, we observed the simultaneous increase of the hydroxide-bound ferric heme *o* and ferric heme *b*. These observations indicate that an electron transfer from the ferrous heme *b* to the ferryl−oxo heme *o* produces the hydroxy intermediate, as found for cytochrome *c* oxidase by resonance Raman studies (*59*−*61*). In the freeze−quenched EPR spectra at 10 and 50 ms, the hydroxide-bound heme *o* signal was persistently observed, but the $g = 3.7$ signal of the pulsed form, which is ascribable to the coupling between ferric heme *o* and cupuric Cu_B (*28*, *62*), was insignificant. Considering the turnover of the enzyme (>500 s^{-1}), the data suggest that the pulsed form may not be an obligate intermediate in dioxygen reduction by cytochrome *bo* under steady-state conditions.

It has been reported that some preparations of cytochrome *bo* contain inhomogeneous components that may display different oxygen reduction kinetics (*30*, *63*). We stress, however, that the observed signals for hemes *b* and *o* cannot be attributed to a possible minor component. We estimated the contents of ferric heme *b* in the time-resolved spectra and found the intensity at 1 ms reaches 60−100% of the whole protein molecule (Figure 5A). It is not possible to quantitate the hydroxy heme *o* due to the spectral overlap; however, the coincidence in the kinetic behaviors of hemes *b* and *o* also suggests that the heme *o* signal is not derived from the minor component.

Dioxygen Reduction by Cytochrome bo without the Bound Q_8. The above mechanism is further confirmed by the observations on the reaction of ΔUbiA. The optical absorption and EPR spectroscopic data demonstrated that heme *b* is oxidized at 0.4 ms in ΔUbiA, implying that heme *b* cannot be rereduced in a single turnover. We therefore interpret that ΔUbiA in the time domain from 0.4 to 1 ms is trapped in the F_I intermediate. While the formation of the hydroxy heme

o was observed at 10 ms, it is significantly slower than that of WT, indicating that the lack of reducing equivalents in ΔUbiA decelerates the formation of the intermediate. The electron donors to make the hydroxy intermediate in ΔUbiA and WT are different, as suggested in the red-shifted Soret absorption spectrum observed for ΔUbiA at 10 ms. Although we could not detect signals arising from a tyrosine radical, a candidate for the electron donor in ΔUbiA is the cross-linked tyrosine.

The comparison of the kinetic absorption and EPR spectra for WT and ΔUbiA and the comparison with the previous experiments (*15*, *27*) confirm the timing of the internal electron transfers associated with the O_2 reduction of cytochrome *bo* (Figure 1). The key feature of the scheme is the stepwise electron transfers from the heme *b*/Q_8 system to the binuclear center that are coupled to the conversions of P to F_I and F_{II} to hydroxy intermediates. The demonstration of the latter coupling is a new finding of this study. Furthermore, the current observations substantiate the reaction mechanism that assumes the absence of the tyrosine radical in the F_I, F_{II}, and hydroxide intermediates, since electrons to generate the F_I and the hydroxy intermediates are supplied from heme *b*. These features are consistent with those of cytochrome *c* oxidase (*44*, *64*) and are important for the understanding of the function of the cross-linked tyrosine residue.

Electronic Structures of the Binuclear Center in the Intermediate States. We intended to observe the EPR signals from the binuclear center in the intermediate states of cytochrome *bo*; however, we could only detect the signals derived from the hydroxy-bound heme *o*. Signals arising from Cu_B(II) or the cross-linked tyrosine radical could not be observed in the current conditions. We inferred that the tyrosine radical is not formed in the intermediate states after F_I as we explained above. In contrast, we have to conclude that Cu_B(II) is EPR silent in these intermediate states. Interestingly, the triple-trap EPR investigation on cytochrome *c* oxidase demonstrated that the P_R intermediate, corresponding to F_I in Figure 1, exhibits a unique EPR signal from Cu_B (*32*). The result is in contrast to the current observation that F_I trapped for ΔUbiA did not show any signals from coppers. Further investigations are necessary to clarify if the discrepancy is caused by the difference in the method of preparing the intermediate states or in the sample sources.

The current results suggest the moderate magnetic interaction between Cu_B and heme *o* in the hydroxide intermediate. The g_x value ($g = 6.9$) observed for the hydroxide-bound heme *o* is smaller than that of the hydroxide-bound high-spin heme in metmyoglobin ($g = 7.3$) (*65*). As indicated in a unique Fe(III)−OH stretching vibration for the hydroxide-bound heme a_3 in cytochrome *c* oxidase (*59*, *65*, *66*), the interaction between heme *o* and Cu_B should be responsible for the smaller g_x value. However, the interaction is weaker than those observed in the pulsed, azide-bound and formate-bound forms of the enzyme, all of which possess a broad signal around $g = 3$ due to the coupling between heme *o* and Cu_B (*28*). We therefore infer that the interaction between heme *o* and Cu_B in the hydroxy intermediate causes only the efficient spin relaxation of Cu_B. Considering that formate and azide bridge between the binuclear center (*28*), we suggest that the hydroxide does not bridge between heme *o* and Cu_B in the hydroxide intermediate.

Summary. Dioxygen reduction by cytochrome *bo*-type quinol oxidase was successfully studied for the first time using the freeze−quench EPR and optical absorption spectroscopies with the submillisecond time resolution. The obtained data can be interpreted on the basis of the reaction scheme, in which the F_I intermediate possessing ferryl−oxo heme *o*, cupric Cu_B, and ferric heme *b* is converted to the F_{II} intermediate by an electron transfer from the bound Q_8H_2 to the ferric heme *b*. Furthermore, it was demonstrated that the conversion of the F_{II} intermediate to the hydroxy intermediate is coupled to the electron transfer from heme *b* to the binuclear center. Finally, it was suggested that the hydroxy intermediate having no bridging ligand between heme *o* and Cu_B is the final intermediate in the catalytic cycle of cytochrome *bo* under steady-state conditions.

ACKNOWLEDGMENT

We thank Dr. R. B. Gennis (University of Illinois) for *E. coli* GO103 and Dr. M. Kawamukai (Shimane University) for *E. coli* MU1227.

REFERENCES

1. Saraste, M., Holm, L., Lemieux, L., Lübben, M., and van der Oost, J. (1991) The happy family of cytochrome oxidases, *Biochem. Soc. Trans. 19*, 608−612.
2. Trumpower, B. L., and Gennis, R. B. (1994) Energy transduction by cytochrome complexes in mitochondrial and bacterial respiration: the enzymology of coupling electron-transfer reactions to transmembrane proton translocation, *Annu. Rev. Biochem. 63*, 675−716.
3. Mogi, T., Tsubaki, M., Hori, H., Miyoshi, H., Nakamura, H., and Anraku, Y. (1998) Two terminal quinol oxidase families in *Escherichia coli*: variations on molecular machinery for dioxygen activation, *J. Biochem., Mol. Biol. Biophys. 2*, 79−110.
4. Hosler, J. P., Ferguson-Miller, S., Calhoun, M. W., Thomas, J. W., Hill, J., Lemieux, L., Ma, J., Georgiou, C., Fetter, J., Shapleigh, J., Tecklenburg, M. M. J., Babcock, G. T., and Gennis, R. B. (1993) Insight into the active-site structure and function of cytochrome oxidase by analysis of site-directed mutants of bacterial cytochrome aa_3 and cytochrome *bo*, *J. Bioenerg. Biomembr. 25*, 121−136.
5. Abramson, J., Riistama, S., Larsson, G., Jasaitis, A., Svensson-Ek, M., Laakkonen, L., Puustinen, A., Iwata, S., and Wikström, M. (2000) The structure of the ubiquinol oxidase from *Escherichia coli* and its ubiquinone binding site, *Nat. Struct. Biol. 2*, 910−917.
6. Yoshikawa, S., Shinzawa-Itoh, K., Nakashima, R., Yaono, R., Yamashita, E., Inoue, N., Yao, M., Fei, M. J., Libeu, C. P., Mizushima, T., Yamaguchi, H., Tomizaki, T., and Tsukihara, T. (1998) Redox-coupled crystal structural changes in bovine heart cytochrome *c* oxidase, *Science 280*, 1723−1729.
7. Buse, G., Soulimane, T., Dewor, M., Meyer, H. E., and Bluggel, M. (1999) Evidence for a copper-coordinated histidine-tyrosine cross-link in the active site of cytochrome oxidase, *Protein Sci. 8*, 985−990.
8. Soulimane, T., Buse, G., Bourenkov, G. P., Bartunik, H. D., Huber, R., and Than, M. E. (2000) Structure and mechanism of the aberrant *ba*(3)-cytochrome *c* oxidase from *Thermus thermophilus*, *EMBO J. 19*, 1766−1776.
9. Iwata, S., Ostermeier, C., Ludwig, B., and Michel, H. (1995) Structure at 2.8 Å resolution of cytochrome *c* oxidase from *Paracoccus denitrificans*, *Nature 376*, 660−669.
10. Tsukihara, T., Aoyama, H., Yamashita, E., Takashi, T., Yamaguchi, H., Shinzawa-Itoh, K., Nakashima, R., Yaono, R., and Yoshikawa, S. (1996) Structures of metal sites of oxidized bovine heart cytochrome *c* oxidase at 2.8 Å resolution, *Science 272*, 1136−1144.
11. Thomson, F., Bailey, J. A., Gennis, R. B., Unkefer, C. J., Li, Z., Silks, L. A., Martinez, R. A., Donohoe, R. J., Dyer, R. B., and Woodruff, W. H. (2002) Direct infrared detection of the covalently ring linked His-Tyr structure in the active site of the heme-copper oxidases, *Biochemistry 41*, 14383−14390.

12. Sato-Watanabe, M., Mogi, T., Ogura, T., Kitagawa, T., Miyoshi, H., Iwamura, H., and Anraku, Y. (1994) Identification of a novel quinone-binding site in the cytochrome *bo* complex from *Escherichia coli*, *J. Biol. Chem. 269*, 28908−28912.
13. Sato-Watanabe, M., Mogi, T., Miyoshi, H., and Anraku, Y. (1998) Characterization and functional role of the Q_H site of *bo*-type ubiquinol oxidase from *Escherichia coli*, *Biochemistry 37*, 5356−5361.
14. Mogi, T., Sato-Watanabe, M., Miyoshi, H., and Orii, Y. (1999) Role of bound ubiquinone on reactions of the *Escherichia coli* cytochrome *bo* with ubiquinol and dioxygen, *FEBS Lett. 457*, 61−64.
15. Svensson-Ek, M., and Brzezinski, P. (1997) Oxidation of ubiquinol by cytochrome bo_3 from *Escherichia coli*: kinetics of electron and proton transfer, *Biochemistry 36*, 5425−5431.
16. Wang, L. C., Rumbley, J., Ching, Y. C., Takahashi, S., Gennis, R. B., and Rousseau, D. L. (1995) Reaction of cytochrome bo_3 with oxygen: extra redox center(s) are present in the protein, *Biochemistry 34*, 15504−15511.
17. Hirota, S., Mogi, T., Ogura, T., Hirano, T., Anraku, T., and Kitagawa, T. (1994) Observation of the Fe−O_2 and Fe(IV)═O stretching Raman bands for dioxygen reduction intermediates of cytochrome *bo* isolated from *Escherichia coli*, *FEBS Lett. 352*, 67−70.
18. Kitagawa, T., and Ogura, T. (1997) Oxygen activation mechanism at the binuclear site of heme copper oxidase superfamily as revealed by time-resolved resonance Raman spectroscopy, *Prog. Inorg. Chem. 45*, 431−479.
19. Chance, B., Saronio, C., and Leigh, J. S. (1975) Functional intermediates in reaction of cytochrome oxidase with oxygen, *J. Biol. Chem. 250*, 9226−9237.
20. Proshlyakov, D. A., Ogura, T., Shinzawa-Itoh, K., Yoshikawa, S., Appelman, E. H., and Kitagawa, T. (1994) Selective resonance Raman observation of the "607 nm" form generated in the reaction of oxidized cytochrome *c* oxidase with hydrogen peroxide, *J. Biol. Chem. 269*, 29385−29388.
21. Uchida, T., Mogi, T., and Kitagawa, T. (2000) Resonance Raman studies of oxo intermediates in the reaction of pulsed cytochrome *bo* with hydrogen peroxide, *Biochemistry 39*, 6669−6678.
22. Morgan, J. E., Verkhovsky, M. I., Puustinen, A., and Wikstrom M. (1995) Identification of a "peroxy" intermediate in cytochrome bo_3 of *Escherichia coli*, *Biochemistry 34*, 15633−15637.
23. Proshlyakov, D. A., Pressler, M. A., DeMaso, C., Leykam, J. F., DeWitt, D. L., and Babcock, G. T. (2000) Oxygen activation and reduction in respiration: involvement of redox-active tyrosine 244, *Science 290*, 1588−1591.
24. MacMillan, F., Kannt, A., Behr, J., Prisner, T., and Michel, H. (1999) Direct evidence for a tyrosine radical in the reaction of cytochrome *c* oxidase with hydrogen peroxide, *Biochemistry 38*, 9179−9184.
25. Blomberg, M. R. A., Siegbahn, P. E. M., Babcock, G. T., and Wikström, M. (2000) Modeling cytochrome oxidase: a quantum chemical study of the O−O bond cleavage mechanism, *J. Am. Chem. Soc. 122*, 12848−12858.
26. Proshlyakov, D. A., Pressler, M. A., and Babcock, G. T. (1998) Dioxygen activation and bond cleavage by mixed-valence cytochrome *c* oxidase, *Proc. Natl. Acad. Sci. U.S.A. 95*, 8020−8025.
27. Puustinen, A., Verkhovsky, M. I., Morgan, J. E., Belevich, N. P., and Wikström, M. (1996) Reaction of the *Escherichia coli* quinol oxidase cytochrome bo_3 with dioxygen: the role of a bound ubiquinone molecule, *Proc. Natl. Acad. Sci. U.S.A. 93*, 1545−1548.
28. Tsubaki, M., Mogi, T., Anraku, Y., and Hori, H. (1993) Structure of the heme-copper binuclear center of the cytochrome *bo* complex of *Escherichia coli*: EPR and Fourier transform infrared spectroscopic studies, *Biochemistry 32*, 6065−6072.
29. Orii, Y., Mogi, T., Sato-Watanabe, M., Hirano, T., and Anraku, Y. (1995) Facilitated intramolecular electron transfer in the *Escherichia coli bo*-type ubiquinol oxidase requires chloride, *Biochemistry 34*, 1127−1132.
30. Svensson-Ek, M., Thomas, J. W., Gennis, R. B., Nilsson, T., and Brzezinski, P. (1996) Kinetics of electron and proton transfer during the reaction of wild type and helix VI mutants of cytochrome bo_3 with oxygen, *Biochemistry 35*, 13673−13680.
31. Mogi, T., Sato-Watanabe, M., Miyoshi, H., and Orii, Y. (1999) Role of a bound ubiquinone on reactions of the *Escherichia coli* cytochrome *bo* with ubiquinol and dioxygen, *FEBS Lett. 457*, 61−64.
32. Morgan, J. E., Verkhovsky, M. I., Palmer, G., and Wikström, M. (2001) Role of P_R intermediate in the reaction of cytochrome *c* oxidase with O_2, *Biochemistry 40*, 6882−6892.
33. Sucheta, A., Szundi, I., and Einarsdottir, O. (1998) Intermediates in the reaction of fully reduced cytochrome *c* oxidase with dioxygen, *Biochemistry 37*, 17905−17914.
34. Brittain, T., Little, R. H., Greenwood, C., and Watmough, N. J. (1996) The reaction of *Escherichia coli* cytochrome *bo* with H_2O_2: evidence for the formation of an oxyferryl species by two distinct routes, *FEBS Lett. 399*, 21−25.
35. Watmough, N. J., Cheesman, M. R., Greenwood, C., and Thomson, A. J. (1994) Cytochrome *bo* from *Escherichia coli*: reaction of the oxidized enzyme with hydrogen peroxide, *Biochem. J. 300*, 469−475.
36. Cheesman, M. R., Watmough, N. J., Gennis, R. B., Greenwood, C., and Thomson, A. J. (1994) Magnetic-circular-dichroism studies of *Escherichia coli* cytochrome *bo*. Identification of high-spin ferric, low-spin ferric and ferryl [Fe(IV)] forms of heme *o*, *Eur. J. Biochem. 219*, 595−602.
37. Moody, A. J., and Rich, P. R. (1994) The reaction of hydrogen peroxide with pulsed cytochrome *bo* from *Escherichia coli*, *Eur. J. Biochem. 226*, 731−737.
38. Rigby, S. E. J., Junemann, S., Rich, P. R., and Heathcote, P. (2000) Reaction of bovine cytochrome *c* oxidase with hydrogen peroxide produces a tryptophan cation radical and a porphyrin cation radical, *Biochemistry 39*, 5921−5928.
39. Rich, P. R., Rigby, S. E. J., and Heathcote, P. (2002) Radicals associated with the catalytic intermediates of bovine cytochrome *c* oxidase, *Biochim. Biophys. Acta 1554*, 137−146.
40. Schultz, B. E., Edmondson, D. E., and Chan, S. I. (1998) Reaction of *Escherichia coli* cytochrome bo_3 with substoichiometric ubiquinol-2: A freeze-quench electron paramagnetic resonance investigation, *Biochemistry 37*, 4160−4168.
41. McCauley, K. M., Vrtis, J. M., Dupont, J., and van der Donk, W. A. (2000) Insights into the functional role of the tyrosine-histidine linkage in cytochrome *c* oxidase, *J. Am. Chem. Soc. 122*, 2403−2404.
42. Cappuccio, J. A., Ayala, I., Elliott, G. I., Szundi, I., Lewis, J., Konopelski, J. P., Barry, B. A., and Einarsdottir, O. (2002) Modeling the active site of cytochrome oxidase: synthesis and characterization of a cross-linked histidine-phenol, *J. Am. Chem. Soc. 124*, 1750−1760.
43. Fabian, M., and Palmer, G. (1995) The interaction of cytochrome oxidase with hydrogen peroxide: the relationship of compounds P and F, *Biochemistry 34*, 13802−13810.
44. Hansson, O., Karlsson, B., Aasa, R., Vanngård, T., and Malmström, B. G. (1982) The structure of the paramagnetic oxygen intermediate in the cytochrome *c* oxidase reaction, *EMBO J. 1*, 1295−1297.
45. Karlsson, B., Aasa, R., Vanngård, T., and Malmström, B. G. (1981) An EPR-detectable intermediate in the cytochrome oxidase−dioxygen reaction, *FEBS Lett. 131*, 186−188.
46. Blair, D. F., Witt, S. N., and Chan, S. I. (1985) Mechanism of cytochrome *c* oxidase-catalyzed dioxygen reduction at low temperatures. Evidence for two intermediates at the three-electron level and entropic promotion of the bond-breaking step, *J. Am. Chem. Soc. 107*, 7389−7399.
47. Moody, A. D., Mitchell, R. H., and Ingledew, W. J. (1990) A gas-flow cryostat for use in freeze-quench studies: design and application to discontinuous pre-steady-state spectral analyses, *Anal. Biochem. 189*, 103−106.
48. Saigo, S., Hashimoto, N., Shibayama, M., Nomura, T., and Nagayama, T. (1993) X-ray absorption spectroscopic studies of a transient intermediate in the reaction of cyanide metmyoglobin with dithionite by using rapid freezing, *Biochim. Biophys. Acta 1202*, 99−106.
49. Tanaka, M., Matsuura, K., Yoshioka, S., Takahashi, S., Ishimori, K., Hori, H., and Morishima, I. (2003) Activation of hydrogen peroxide in horseradish peroxidase occurs within ∼200 μs observed by a new freeze-quench device, *Biophys. J. 84*, 1998−2004.
50. Mogi, T., Hirano, T., Nakamura, H., Anraku, Y., and Orii, Y. (1995) Cu_B promotes both binding and reduction of dioxygen at the heme-copper binuclear center in the *Escherichia coli bo*-type ubiquinol oxidase, *FEBS Lett. 370*, 259−263.
51. Antonini, E., and Brunori, M. (1971) *Hemoglobin and Myoglobin in Their Reactions with Ligands*, American Elsevier Publishing Co., New York.

52. Hunter, D. J. B., Moody, A. J., Rich, P. R., and Ingledew, W. J. (1997) EPR spectroscopy of *Escherichia coli* cytochrome *bo* which lacks Cu_B, *FEBS Lett. 412*, 43−47.
53. Gurd, F. R. N., Falk, K.-E., Malmström, B. G., and Vänngård, T. (1967) A Magnetic resonance study of sperm whale ferrimyoglobin and its complex with 1 cupric ion, *J. Biol. Chem. 242*, 5724−5730.
54. Ingledew, W. J., Ohnishi, T., and Salerno, J. C. (1995) Studies on a stabilization of ubisemiquinone by *Escherichia coli* quinol oxidase, cytochrome *bo*, *Eur. J. Biochem. 227*, 903−908.
55. Sato-Watanabe, M., Itoh, S., Mogi, T., Matsuura, K., Miyoshi, H., and Anraku, Y. (1995) Stabilization of a semiquinone radical at the high-affinity quinone-binding site (Q_H) of the *Escherichia coli bo*-type ubiquinol oxidase, *FEBS Lett. 374*, 265−269.
56. Wikström, M. (1981) Energy-dependent reversal of the cytochrome oxidase reaction, *Proc. Natl. Acad. Sci. U.S.A. 78*, 4051−4054.
57. Wikström, M., and Morgan, J. E. (1992) The dioxygen cycle. Spectral, kinetic, and thermodynamic characteristics of ferryl and peroxy intermediates observed by reversal of the cytochrome oxidase reaction, *J. Biol. Chem. 267*, 10266−10273.
58. Kobayashi, K., Tagawa, S., and Mogi, T. (2000) Transient formation of ubisemiquinone radical and subsequent electron-transfer process in the *Escherichia coli* cytochrome *bo*, *Biochemistry 39*, 15620−15625.
59. Han, S., Ching, Y., and Rousseau, D. L. (1990) Ferryl and hydroxy intermediates in the reaction of oxygen with reduced cytochrome *c* oxidase, *Nature 348*, 89−91.
60. Ogura, T., Hirota, S., Proshlyakov, D. A., Shinzawa-Itoh, K., Yoshikawa, S., and Kitagawa, T. (1996) Time-resolved resonance Raman evidence for tight coupling between electron transfer and proton pumping of cytochrome *c* oxidase upon the change from the Fe(V) oxidation level to the Fe(IV) oxidation level, *J. Am. Chem. Soc. 118*, 5443−5449.
61. Han, S., Takahashi, S., and Rousseau, D. L. (2000) Time dependence of the catalytic intermediates in cytochrome *c* oxidase, *J. Biol. Chem. 275*, 1910−1919.
62. Tsubaki, M., Hori, H., and Mogi, T. (2000) Probing molecular structure of dioxygen reduction site of bacterial quinol oxidases through ligand binding to the redox metal centers, *J. Inorg. Biochem. 82*, 19−25.
63. Bailey, J. A., Tomson, F. L., Mechlenburg, S. L., MacDonald, G. M., Katsonouri, A., Puustinen, A., Gennis, R. B., Woodruff, W. H., and Dyer, R. B. (2002) Time-resolved step-scan Fourier transform infrared spectroscopy of the CO adducts of bovine cytochrome *c* oxidase and of cytochrome bo_3 from *Escherichia coli*, *Biochemistry 41*, 2675−2683.
64. Van Eps, N., Szundi, I., and Einarsdóttir, Ó. (2000) A new approach for studying fast biological reactions involving dioxygen: the reaction of fully reduced cytochrome *c* oxidase with O_2, *Biochemistry 39*, 14576−14582.
65. Asher, S. A., Vickery, L. E., Schuster, T. M., and Sauer, K. (1977) Resonance Raman spectra of methemoglobin derivatives. Selective enhancement of axial ligand vibrations and lack of an effect of inositol hexaphosphate, *Biochemistry 26*, 5849−5856.
66. Feis, A., Marzocchi, M. P., Paoli, M., and Smulevich, G. (1994) Spin state and axial ligand bonding in the hydroxide complexes of metmyoglobin, methemoglobin, and horseradish peroxidase at room and low temperatures, *Biochemistry 33*, 4577−4583.

BI0355490